Usefulness of Body Composition CT Analysis in Patients with Idiopathic Pulmonary Fibrosis: A Pilot Study

Carole Jalaber, Jeanne Lemerre-Poincloux, Stéphane Jouneau, Chloé Rousseau, Bertrand Dolou, Eddy Rouag, Alain Lescoat, David Luque-Paz, Charlotte Lucas, Laurent Vernhet, et al.

Version of Record: https://www.sciencedirect.com/science/article/pii/S1076633221003287
Manuscript_99974c3a60a4fab4c0b151863adabef6

Usefulness of body composition CT analysis in patients with idiopathic pulmonary fibrosis: a pilot study

Carole Jalaber (1), Jeanne Lemerre-Poincloux (2), Stéphane Jouneau (3, 4), Chloé Rousseau (5), Bertrand Dolou (2), Eddy Rouag (6), Alain Lescoat (7, 4), David Luque-Paz (8), Charlotte Lucas (9), Laurent Vernhet (4), Ronan Thibault (10,11), Mathieu Lederlin (2,12)

Affiliations:

(1) Department of Radiology, Saint-Etienne University Hospital, Saint-Etienne, F-42000, France
(2) Department of Radiology, Rennes University Hospital, Rennes, F- 35000, France
(3) Department of Respiratory Diseases, Rennes University Hospital, Rennes, F- 35000, France
(4) Univ Rennes, INSERM, EHESP, IRSET UMR S1085, Rennes, France
(5) Clinical Investigation Center INSERM 1414, Clinical Pharmacology Service, University Hospital, Rennes, France
(6) GE Healthcare France, 283 rue de la Minière, Buc 78530, France
(7) Department of Internal Medicine and Clinical Immunology, Rennes University Hospital, Rennes, F- 35000, France.
(8) Infectious Diseases and Intensive Care Unit, University Hospital of Rennes, Rennes, France
(9) Department of rheumatology, Rennes University Hospital, Rennes, F- 35000, France
(10) Nutrition Unit, University Hospital of Rennes, F- 35000, France
(11) INRAE, INSERM, Univ Rennes, Nutrition Metabolisms and Cancer, NuMeCan, Rennes, France
(12) Univ Rennes, INSERM, LTSI, UMR 1099, Rennes, France

Corresponding author:

Mathieu Lederlin, Department of radiology, University Hospital of Rennes, University of Rennes, 2 rue Henri le Guilloux, 35000 Rennes, France. Telephone number : + 33 2 99 28 25 23, email : mathieu.lederlin@chu-rennes.fr

Conflict of interest statement

S.J. has received fees, funding or reimbursement for national and international conferences, boards, expert or opinion groups, research projects over the past 5 years from Actelion, AIRB, Astra Zeneca, Bellorophon Therapeutics, Biogen, BMS, Boehringer Ingelheim, Chiesi, Fibrogen, Galecto Biotech, Genzyme, Gilead, GSK, LVL, Mundipharma, Novartis, Olam Pharm, Pfizer, Pliant Therapeutics, Roche, Sanofi, Savara-Serendex.

R.T. has received royalties for designing the Simple Evaluation of Food Intake® (SEFI®) tool (Knoë, le Kremlin Bicêtre, France), and consulting fees from F. Hoffmann-La Roche, Ltd.

M.L. has received consulting fees over the past 5 years from Astra Zeneca, Boehringer Ingelheim, Siemens Healthineers.

C.J., J.L-P., C.R., B.D., E.R., A.L., D.L-P., C.L., L.V. none

Usefulness of body composition CT analysis in patients with idiopathic pulmonary fibrosis: a pilot study

Abstract

Purpose: To evaluate the feasibility of a chest CT-based body composition analysis in idiopathic pulmonary fibrosis (IPF), and to investigate the respective contribution of lung and muscle CT quantitative analyses to the prognosis of IPF.

Method: A total of 71 IPF patients were recruited at diagnosis. All patients underwent a standard chest CT-scan and a bioelectrical impedance analysis considered as reference standard for estimating malnutrition through the use of the fat-free mass index (FFMI). The skeletal muscle index (SMI) was measured on chest-CT at the level of the first lumbar vertebra by two radiologists. Lung fibrosis extent was quantified by three radiologists in consensus. The extent of emphysema, the pulmonary artery to aorta (PA/AO) diameter ratio and lymph node enlargement were also reported. Mortality and hospitalization over a 14-month follow-up were recorded.

Results: A low FFMI defining malnutrition was identified in 26.8% of patients. SMI was significantly lower in these patients ($P<0.001$) and was correlated with FFMI ($r=0.637$, $P<0.001$). Interobserver agreement of SMI measurement was very good (ICC=0.91). For diagnosing malnutrition, SMI showed a 0.79 sensitivity, a 0.69 specificity, a 0.48 PPV and a 0.90 NPV. In univariate analysis, fibrosis extent was significantly associated with death, while SMI did not reach significance. In multivariate analysis, fibrosis extent and PA/AO ratio were independently associated with hospitalization.

Conclusions: SMI measured on chest CT could be a reliable tool to exclude malnutrition in IPF. A quantitative analysis of both fibrosis and skeletal muscle may allow holistic management of IPF patients.

Keywords

Idiopathic pulmonary fibrosis

Chest CT

Malnutrition

Bioelectrical impedance analysis

Skeletal muscle index

Abbreviations

BIA: bioelectrical impedance analysis

COPD: Chronic obstructive pulmonary disease

CT: computerized tomography

DLCO: carbon monoxide diffusing capacity

FFMI: fat-free mass index

FMI: fat mass index

FVC: forced vital capacity

GAP: Gender-Age-Physiology index

IPF: Idiopathic pulmonary fibrosis

NPV: negative predictive value

PA/AO: main pulmonary artery to ascending aorta ratio

PFT: pulmonary functional test

PPV: positive predictive value

SMA: skeletal muscle area

SMI: skeletal muscle mass index

Introduction

Idiopathic pulmonary fibrosis (IPF) is a severe chronic interstitial lung disease with a 5-year survival rate of approximately 40% (1,2). While decreased forced vital capacity (FVC) is considered the most important prognostic marker in clinical trials (3–5), chest CT plays an essential role in the diagnosis and follow-up of IPF patients. Chest CT is not only the mainstay of IPF diagnosis, but CT extent of lung fibrosis is also strongly associated with mortality in IPF patients (6,7).

In addition to lung involvement, other conditions may influence the prognosis of patients with IPF. In the past few years, body weight loss and malnutrition have been associated with a reduction of overall survival in IPF (8–11). Nutritional status can be explored, beyond the use of body mass index (BMI) or waist circumference, through the analysis of body composition allowing the quantification of body's core components such as fat mass and fat-free mass including skeletal muscle tissue. The bioelectrical impedance analysis (BIA) is a simple and validated technique for body composition analysis (12–14). The measurement of the fat-free mass index (FFMI) is a phenotypic diagnostic criterion of malnutrition (15), which could identify a decrease in skeletal muscle mass. In IPF, a low FFMI has been recognized as an independent risk factor for mortality (16,17).

Recently, several groups have studied a biomarker called skeletal muscle index (SMI), which was measured and calculated from CT slices of the upper abdomen at the third lumbar vertebra (L3) especially in cancer patients, and which was found to correlate with markers of malnutrition including FFMI (18). At the thoracic level, SMI has only been investigated in a few studies on chronic obstructive pulmonary disease or lung carcinoma (19,20).

The objectives of the present study were to evaluate the feasibility of a CT-based body composition analysis at the thoracic level in IPF, and to investigate the prognostic value of lung and muscle CT biomarkers in IPF patients.

Methods

Study design and patient recruitment

This retrospective single-center observational study used prospective data collection of patients referred by general hospitals to the tertiary referral center for IPF at the University Hospital of Rennes (CHU Rennes). We included all consecutive patients diagnosed with IPF according to the ATS/ERS/JRS/ALAT consensus criteria between May 2016 and November 2018. Inclusion criteria were: all incident patients having both chest CT and BIA examinations performed less than 3 months apart. Non-inclusion criteria were: patients with evidence of acute unstable disease or confounding respiratory event either clinically or at CT-scan (*e.g.* infection or IPF acute exacerbation), non-availability of CT datasets reconstructed with both standard and lung kernels, or CT images of insufficient quality (*e.g.* severe breathing artifacts).

Data Collection

Clinical data including age, gender, smoking history, comorbidities, dyspnea and cough were obtained from electronic medical records. Pulmonary function tests (PFT) including forced vital capacity (FVC) and carbon monoxide diffusing capacity (DLCO) were performed in accordance with ATS/ERS guidelines (21). FVC and DLCO were expressed as % of predicted value according to the European reference equations (22). The Gender-Age-Physiology (GAP) index was calculated using gender, age, FVC and DLCO as proposed by Ley et al (23). The nutritional status of patients was clinically assessed using the following parameters: height, weight, BMI calculated as weight/height² (kg/m²), mid-arm circumference (MAC), triceps skinfold thickness (TSF), mid-arm muscular circumference (MAMC) calculated as: MAC – (π x TSF). Food intake was assessed using the 10-point visual analogue scale of the Simplified Evaluation of Food Intake (SEFI®) (www.sefi-nutrition.com) (24,25). Serum

albumin, pre-albumin and C-reactive protein (CRP) were recorded for all patients. Clinical outcome including all-cause mortality or lung transplantation and all-cause hospitalization were collected until January 2020 to ensure a minimal follow-up of 14 months for all patients.

Bioelectrical impedance analysis

BIA has become a standard of care in our center since 2016 in the initial diagnosis and follow-up of patients with IPF. Body composition was assessed using BIA carried out on a multifrequency bioimpedance generator/analyzer (Quadscan 4000, Bodystat Ltd, Isle of Man, UK). The body composition parameters recorded for the study were FFMI, fat mass index (FMI) and phase angle, which is a marker of cellular integrity and nutritional status associated with mortality (26).

CT protocol

CT examinations were performed in a routine care setting by using 64- or more detector row CT scanners (Somatom Force, Siemens Healthcare, Forchheim, Germany; Aquilion Prime; Canon Medical Systems, Tustin, CA, USA; Discovery CT 750 HD, GE Healthcare, Milwaukee, WI, USA). All patients had non-enhanced chest CT scan acquired in volumetric mode and submillimeter collimation from thoracic inlet to lung bases in suspended full inspiration using standard parameters. Typical acquisition parameters were: tube voltage 120 kV, tube current 90-230 mAs with a dose modulation protocol, gantry rotation 0.3-0.4 second, spiral pitch factor 0.9-2.3. CT images were reconstructed at section widths of 0.625 to 1.25 mm using both standard soft tissue and high spatial frequency algorithms. Volume CT dose index (CTDIvol) ranged from 0.8 to 9.25 mGy, and dose-length product (DLP) ranged from 84 to 324 mGy.cm.

CT-based quantitative analysis of skeletal muscle

For skeletal muscle analysis, CT images were visualized using mediastinal window (level, 50 Hounsfield Units (HU); width, 350 HU). A preliminary analysis (see supplemental Methods, Table S1, Figures S1 and S2) had previously defined the first lumbar vertebra (L1) level as the most relevant level for skeletal muscle segmentation. For all patients, skeletal muscle area (SMA in cm^2) was quantified on a single CT slice reconstructed with soft tissue kernel algorithm at the L1 level using AW Server 3.2 (GE Healthcare, Chicago, IL, USA). After selection of a suitable CT slice at the L1 level, a threshold segmentation algorithm (-29 to 150 HU) was applied to include skeletal muscle (27). This automatic segmentation was followed by manual correction to exclude all pixels not corresponding to skeletal muscle, and thus keep only SMA including *transversospinalis, erector spinae, serratus posterior, latissimus dorsi* and intercostal muscles (Figure 1). Then the SMI (cm^2/m^2) was calculated as SMA normalized by height squared.

Two radiologists with 4 years of experience in thoracic imaging independently performed muscle analysis blinded to the patients' nutritional status. Each was required to select the L1 slice of their choice, then apply automatic thresholding and perform manual segmentation to derive the SMI. The pairs of SMI values were used to assess interobserver agreement, whereas the means of the paired values were used for subsequent analyses.

CT-based quantitative analysis of pulmonary features

Three radiologists (the two previous ones plus a radiologist with 18 years of experience in chest imaging) performed pulmonary analysis on CT images reconstructed with lung kernel algorithm blinded to clinical and spirometric data. CT images were reviewed on a commercial Picture Archiving and Communication System (PACS; Telemis PACS-software, version 4.7, Telemis SA, Louvain-la-Neuve, Belgium), using lung window (level, -650 HU; width, 1500

HU). An initial training session was conducted with all readers. The three radiologists independently quantified the total extent of fibrosis and emphysema, rounded to the nearest 5%, using a previously published method (6). Fibrosis areas were defined as reticular opacities and honeycombing. Emphysema was defined as focal areas of low attenuation without visible walls. For both fibrosis and emphysema, if there was a discrepancy of more than 20% between the three radiologists, the case was reviewed and a consensus was reached. In addition, one radiologist reported the presence of lymph node enlargement (defined as short-axis diameter exceeding 10mm), esophageal dilatation, and the main pulmonary artery to ascending aorta (PA/AO) diameter ratio.

Statistical Analysis

Quantitative variables were expressed as mean ± SD or median and interquartile range according to their distribution, and categorical variables as number of patients or frequency (%).

The comparisons between groups (patients with low FFMI vs patients with normal/high FFMI) were performed using Student's t-test (or Mann–Whitney–Wilcoxon / Kruskall Wallis test when appropriate) for continuous data, and $\chi 2$ tests (or Fisher's exact test when appropriate) for categorical data.

After checking the normality of SMI, interobserver agreement was studied analytically by calculating the intra-class correlation coefficient (ICC) and graphically by using the Bland-Altman method (28). ICC were considered poor < 0.20; fair from 0.20 to 0.39; moderate from 0.40 to 0.59; good from 0.60 to 0.79; excellent ≥ 0.80 (29). Correlation between SMI and both nutritional and respiratory markers was assessed using Spearman's and Pearson tests.

Receiver operating characteristic (ROC) curve analysis was used to assess the diagnostic performance of SMI compared to FFMI, considered as the reference standard for estimating

skeletal muscle loss (12,13). FFMI was considered to be low when it was below 17 kg/m² in men and below 15 kg/m² in women (15). Optimal thresholds were calculated by maximizing the Youden index. Associated sensitivity, specificity, positive predictive value (PPV) and negative predictive value (NPV) were computed with their 95 % confidence interval (CI). ROC curves were analyzed with their area under the curve (AUC) and 95 % CI. The discriminative power of the AUC was defined as: $0.60 \leq AUC < 0.70$, fair; $0.70 \leq AUC < 0.80$, acceptable; $0.80 \leq AUC < 0.90$, excellent; $0.90 \leq AUC < 1$, outstanding (30).
Variables available in routine clinical practice that may affect death or transplantation, and hospitalization, were tested in univariate Cox proportional hazard models. The significant variables ($P<0.20$) of the univariate analysis were included in a final multivariate model which was constructed using a stepwise backward selection method.
All analyses were performed using SAS software version 9.4 (SAS Institute Inc., Cary, NC, USA), and two-tailed P values of <0.05 were considered statistically significant.

This study was approved by the institutional ethics board of Rennes University Hospital, France (N 17.53).

Results

Patient characteristics

A total of 71 patients met the inclusion criteria and were recruited on the study period. The flowchart of the population is provided in Figure 2.
The mean delay between BIA and chest CT-scan was 35.4 ± 25.6 days. Patients' characteristics are presented in Table 1. The mean age of the patients was 74.1 ± 7.5 years, with 76.1% (54/71) of them being male. The mean FVC was 81 ±17% and the mean DLCO

was 46 ± 14% of the predicted values. The mean BMI was 27.3 ± 3.8 kg/m². Chest CT mean fibrosis score was 28 ± 12% and mean emphysema score was 4 ± 7%.

The mean FFMI was 19.1 ± 2.1 kg/m² in men and 14.7 ± 2.2 kg/m² in women. A low FFMI (*i.e.* loss of skeletal muscle mass) was identified in 26.8% (19/71) of patients and was more prevalent in women and non-smokers (P=0.010 and P=0.003, respectively). Differences in patient characteristics according to FFMI are presented in Table 1. A low FFMI was associated with lower DLCO value (%pred) (P=0.010) but not with lower FVC value (%pred) (P=0.328). Patients with low FFMI had significantly lower BMI and MAMC than those with normal/high FFMI (P<0.001), as well as lower phase angle at BIA (P=0.001). There was no difference in fibrosis score between low and normal/high FFMI patients (32.8 ± 11.6% vs 26.6 ± 12.4%, respectively; P=0.062). SMI was significantly lower in patients with low FFMI compared to those with normal or high FFMI (40.1 ± 7 cm²/m² vs 48.4 ± 6.9 cm²/m², respectively; P<0.001).

SMI interobserver agreement

Interobserver agreement of SMI measurement was very good with an ICC of 0.91 (95% CI: 0.85-0.94). Bland-Altman analysis (Figure 3) showed a mean bias of 2.7 cm²/m² with limits of agreement ranging from -1.5 to 6.8 cm²/m² (95% CI: -2.4 to -0.6 and 6.0 to 7.7 cm²/m², respectively).

Correlation between SMI and parameters of nutritional status

SMI was significantly correlated with FFMI (r=0.637, P<0.001), BMI (r=0.579, P<0.001) and MAMC (r=0.497, P<0.001). There was no significant correlation between SMI and TSF, SEFI, albumin, pre-albumin, CRP, FMI and phase angle (Table 2).

Correlation between SMI and respiratory parameters

SMI was significantly correlated with DLCO (r=0.347, P=0.006). There was no significant correlation between SMI and FVC, fibrosis score and emphysema score (Table 2).

Diagnostic performance of SMI for low FFMI

Separate ROC analyses in males and females resulted in optimal SMI threshold values of 47.4 cm^2/m^2 and 35 cm^2/m^2 for defining skeletal muscle loss, *i.e.* low FFMI, respectively (Table 3). By using these gender-based threshold values of SMI, the area under the ROC curve was 0.80 (95% CI, 0.68–0.91) with a sensitivity of 0.79 (95% CI, 0.61–0.97), a specificity of 0.69 (95% CI, 0.57–0.82), a PPV of 0.48 (95% CI, 0.31–0.66) and a NPV of 0.90 (95% CI, 0.81–0.99) (Figure 4, Table 3).

Variables associated with clinical outcomes

The median follow-up was 23.4 months, excluding four patients who were lost to follow-up. During the follow-up period, 20 patients (30%) died or were transplanted, and 25 (37%) were hospitalized.

In univariate analysis, the variables significantly associated with death or transplantation were: higher age (P=0.008), lower FVC (P=0.001), lower DLCO (P=0.003) and higher fibrosis score (P=0.007), but not BMI (P=0.080) or SMI (P=0.091). In multivariate analysis, only DLCO (%pred) was independently associated with death or transplantation (P=0.026) (Table 4).

In univariate analysis, the variables significantly associated with hospitalization were: lower DLCO (%pred) (P=0.020), higher fibrosis score (P=0.039), lymph node enlargement (P=0.023) and higher PA/AO ratio (P=0.014), but not BMI (P=0.225) or SMI (P=0.276). In multivariate analysis, a higher fibrosis score (P=0.0078) and a higher PA/AO ratio (P=0.0065)

were independently associated with hospitalization (Table 5). Typical examples are shown in Figures 5 and 6.

Discussion

In this study, we showed that measuring SMI on a chest CT at the L1 level is a reliable method to assess malnutrition in IPF patients. In clinical routine, BMI is a widely used index to define normal weight, overweight and underweight (31). A BMI <18.5 and weight loss could be in favor of malnutrition status, but do not account for the proportion and the distribution of adipose and lean tissue masses. Although BIA is one of the reference methods to assess body composition, CT scan also allows such an estimation. A decrease of SMI below the cut-off of normal values could be a good surrogate marker of malnutrition (32). Two groups recently quantified *pectoralis* and *erector spinae* muscles from different chest CT slices (4^{th} and 12^{th} vertebra levels), but they included prevalent and not incident patients, and CT parameters of body composition were not compared to the usual diagnostic criteria of malnutrition (33,34).

SMI is a robust and reproducible parameter, which can be derived whether CT is performed with or without contrast medium injection (35,36). It has been widely validated on abdominal CT scan at the L3 level (18). Since the L3 level is generally not included within a chest CT dataset, our objective was to transpose the calculation of SMI to the thoracic level through a validated approach: (i) identification of the most appropriate level to measure SMI on chest CT, (ii) assessment of interobserver agreement, (iii) calculation of the correlation between SMI and FFMI. With an ICC of 0.91, the interobserver agreement of SMI was very good, in line with previous studies (37,38). As demonstrated by Perthen et al, the main source of variability is likely to be the choice of the slice by each observer, since the height of the L1 vertebra is about 2cm (37). The threshold values of SMI we used to define loss of skeletal

muscle (47 cm^2/m^2 in men and 35 cm^2/m^2 in women) are similar to those found in cancer studies, either at L1 level (46 and 29 cm^2/m^2, respectively (39)) or at L3 level (52 and 39 cm^2/m^2, respectively (40)). Based on these threshold values, we found a 50% PPV, suggesting that SMI should not be used as a stand-alone test to screen for malnutrition in IPF. On the other hand, the 90% NPV suggests that SMI could be used to exclude malnutrition in IPF patients, although larger studies and external validation are needed to confirm these results. Our study also suggests that a quantitative analysis of both lung parenchyma and skeletal muscle may have prognostic value in IPF patients. The fibrosis score was significantly associated with the risk of death and, independently, with the risk of hospitalization, which is consistent with previous study results (3,7). Lymph node enlargement was also associated with hospitalization in univariate analysis, which is in agreement with previous studies (41–44). This is a common feature in IPF patients (55 to 70% of cases) that is thought to be related to a high immunologic response involving the recruitment of T cells from the peripheral circulation through lymph nodes to the lungs, thus contributing to the development of pulmonary fibrosis (45).

The SMI showed a trend towards an association with the risk of death, which did not reach significance. This could be due to a lack of power related to insufficient sample size. The BMI was also not associated with key prognostic outcomes in our cohort (death/transplant or hospitalization) while it was reported to be a predictive factor in IPF (9,46). The mechanisms underlying malnutrition in IPF are multiple and still poorly understood: reduced physical activity due to decreased lung function, systemic inflammation, digestive disorders related to treatment. Future studies will need to address the question of whether SMI is a more specific marker of malnutrition than BMI in IPF. Moreover, as weight loss during follow-up is a diagnostic criterion for malnutrition independently from BMI (9,15,46), it could be relevant to analyze whether the longitudinal variation in SMI over two successive CT exams is a better

diagnostic criterion for malnutrition than a single baseline SMI assessment. Since the publication of the INBUILD trial (47), the concept of "progressive" fibrosing interstitial lung disease has become a key element in the decision to treat. This concept might be transposed to malnutrition, assuming that a decrease in SMI may be more sensitive to predict patient outcomes. The ultimate goal would be to propose, in addition to anti-fibrotic agents, intervention program based on nutritional support and physical exercise.

In this study, we described a routine approach to extract a simple nutritional parameter from any workstation in less than 5 minutes. One of the strengths of this study is that all patients underwent BIA, a validated method for estimating skeletal muscle mass. Based on BIA, we could propose new SMI thresholds to define low skeletal muscle mass in IPF patients. In addition, all patients were recruited at diagnosis prior to any treatment at the time of the investigations. As antifibrotic agents can cause gastrointestinal adverse effects or anorexia, thus potentially contributing to malnutrition, we were able to avoid such analytical bias.

The main limitation of the study is the small sample size, which, as mentioned above, may have limited the statistical power of the analyses. This is related to the monocentric nature of the study but also to the selective inclusion criteria, which comprised chest CT and BIA examinations, both performed at diagnosis, less than 3 months apart. There are also limitations inherent to the retrospective nature of the study including missing data. Because of these limitations, SMI thresholds are proposals that will deserve to be validated on a larger scale. Finally, CT analysis of muscle and lung was done manually. This is not a major flaw for SMI assessment as it was largely computer-aided and showed excellent interobserver agreement. It is more questionable for fibrosis which was visually assessed through a semi-quantitative method. Even if our quantification required a triple consensus, it is known that visual analysis lacks reproducibility (48). However, current automatic post-processing tools are still insufficiently standardized to reliably quantify fibrosis lesions (49). In the near future,

deep learning-based algorithms could offer fully automated approaches to quantify both lung fibrosis and skeletal muscle from CT-scans (50,51).

To conclude, the concomitant evaluation of lung and skeletal muscle on a chest CT scan may provide new meaningful information for the management of IPF in the future. Specifically, the use of SMI thresholds proposed here is associated with a satisfactory negative predictive value. Although it requires external validation, SMI may therefore be useful to exclude malnutrition in IPF patients. It remains to be determined whether SMI is a more specific marker of malnutrition than BMI, and whether it is a prognostic factor independent from the extent of pulmonary fibrosis.

References

1. Ley B, Collard HR, King TE. Clinical Course and Prediction of Survival in Idiopathic Pulmonary Fibrosis *Am J Respir Crit Care Med* 2011;183:431-40.

2. Alakhras M, Decker PA, Nadrous HF, et al. Body Mass Index and Mortality in Patients With Idiopathic Pulmonary Fibrosis. *Chest* 2007;131:1448-53.

3. Best AC, Meng J, Lynch AM, et al. Idiopathic Pulmonary Fibrosis: Physiologic Tests, Quantitative CT Indexes, and CT Visual Scores as Predictors of Mortality. *Radiology* 2008;246:935-40.

4. Flaherty KR, Mumford JA, Murray S, et al. Prognostic Implications of Physiologic and Radiographic Changes in Idiopathic Interstitial Pneumonia. *Am J Respir Crit Care Med* 2003;168:543-8.

5. Zappala CJ, Latsi PI, Nicholson AG, et al. Marginal decline in forced vital capacity is associated with a poor outcome in idiopathic pulmonary fibrosis. *European Respiratory Journal* 2010;35:830-6.

6. Ley B, Elicker BM, Hartman TE, et al. Idiopathic Pulmonary Fibrosis: CT and Risk of Death. *Radiology* 2014;273:570-9.

7. Sumikawa H, Johkoh T, Colby TV, et al. Computed Tomography Findings in Pathological Usual Interstitial Pneumonia: Relationship to Survival. *Am J Respir Crit Care Med* 2008;177:433-9.

8. Kulkarni T, Yuan K, Tran-Nguyen TK, et al. Decrements of body mass index are associated with poor outcomes of idiopathic pulmonary fibrosis patients. *PLoS ONE* 2019;14:e0221905.

9. Nakatsuka Y, Handa T, Kokosi M, et al. The Clinical Significance of Body Weight Loss in Idiopathic Pulmonary Fibrosis Patients. *Respiration* 2018;96:338-47.

10. Pugashetti J, Graham J, Boctor N, et al. Weight loss as a predictor of mortality in patients with interstitial lung disease. *Eur Respir J* 2018;52:1801289.

11. Jouneau S, Lederlin M, Vernhet L, et al. Malnutrition in idiopathic pulmonary fibrosis: the great forgotten comorbidity! *Eur Respir J* 2019;53:1900418.

12. Kyle UG, Bosaeus I, De Lorenzo AD, et al. Bioelectrical impedance analysis—part I: review of principles and methods. Clinical Nutrition 2004;23:1226-43.

13. Kyle UG, Bosaeus I, De Lorenzo AD, et al. Bioelectrical impedance analysis—part II: utilization in clinical practice. Clinical Nutrition 2004;23:1430-53.

14. Thibault R, Genton L, Pichard C. Body composition: Why, when and for who? *Clinical Nutrition* 2012;31:435-47.

15. Cederholm T, Jensen GL, Correia MITD, et al. GLIM criteria for the diagnosis of malnutrition – A consensus report from the global clinical nutrition community. *Clinical Nutrition* 2019;38:1-9.

16. Nishiyama O, Yamazaki R, Sano H, et al. Fat-free mass index predicts survival in patients with idiopathic pulmonary fibrosis: Fat-free mass index in IPF. *Respirology* 2017;22:480-5.

17. Jouneau S, Kerjouan M, Rousseau C, et al. What are the best indicators to assess malnutrition in idiopathic pulmonary fibrosis patients? A cross-sectional study in a referral center. *Nutrition* 2019;62:115-21.

18. Shen W, Punyanitya M, Wang Z, et al. Total body skeletal muscle and adipose tissue volumes: estimation from a single abdominal cross-sectional image. *Journal of Applied Physiology* 2004;97:2333-8.

19. Costa TM da RL, Costa FM, Moreira CA, et al. Sarcopenia in COPD: relationship with COPD severity and prognosis. *J bras pneumol* 2015;41:415-21.

20. Recio-Boiles A, Galeas JN, Goldwasser B, et al. Enhancing evaluation of sarcopenia in patients with non-small cell lung cancer (NSCLC) by assessing skeletal muscle index (SMI) at the first lumbar (L1) level on routine chest computed tomography (CT). *Support Care Cancer* 2018;26:2353-9.

21. Miller MR. General considerations for lung function testing. *European Respiratory Journal* 2005;26:153-61.

22. Pellegrino R. Interpretative strategies for lung function tests. *European Respiratory Journal*. 2005;26:948-68.

23. Lee SH, Kim SY, Kim DS, et al. Predicting survival of patients with idiopathic pulmonary fibrosis using GAP score: a nationwide cohort study. *Respir Res* 2016;17:131.

24. Thibault R, Goujon N, Le Gallic E, et al. Use of 10-point analogue scales to estimate dietary intake: A prospective study in patients nutritionally at-risk. *Clinical Nutrition* 2009;28:134-40.

25. Bouëtté G, Esvan M, Apel K, et al. A visual analogue scale for food intake as a screening test for malnutrition in the primary care setting: Prospective non-interventional study. *Clinical Nutrition* 2021;40:174-80.

26. Thibault R, Makhlouf A-M, Mulliez A, et al. Fat-free mass at admission predicts 28-day mortality in intensive care unit patients: the international prospective observational study Phase Angle Project. *Intensive Care Med* 2016;42:1445-53.

27. Martin L, Birdsell L, MacDonald N, et al. Cancer Cachexia in the Age of Obesity: Skeletal Muscle Depletion Is a Powerful Prognostic Factor, Independent of Body Mass Index. *JCO* 2013;31:1539-47.

28. Bland JM, Altman DG. Statistical methods for assessing agreement between two methods of clinical measurement. *Lancet* 1986;1:307-10.

29. Shrout PE, Fleiss JL. Intraclass correlations: uses in assessing rater reliability. *Psychol Bull* 1979;86:420-8.

30. Hosmer, D.W., Lemeshow, S. : Applied logistic regression. *New York* 2000. doi:10.1002/0471722146

31. Evans WJ, Morley JE, Argilés J, et al. Cachexia: A new definition. *Clinical Nutrition* 2008;27:793-9.

32. Albano D, Messina C, Vitale J, et al. Imaging of sarcopenia: old evidence and new insights. *Eur Radiol* 2020;30:2199-208.

33. Moon, S., Choi, J., Lee, S. et al. Thoracic skeletal muscle quantification : low muscle mass is related with worse prognosis in idiopathic pulmonary fibrosis patients. *Respir Res* 20, 35 (2019). https://doi.org/10.1186/s12931-019-1001-6

34. Awano N, Inomata M, Kuse N, et al. Quantitative computed tomography measures of skeletal muscle mass in patients with idiopathic pulmonary fibrosis according to a multidisciplinary discussion diagnosis: a retrospective nationwide study in Japan. *Respir Investig* 2020;58:91-101.

35. Mourtzakis M, Prado CMM, Lieffers JR, et al. A practical and precise approach to quantification of body composition in cancer patients using computed tomography images acquired during routine care. *Appl Physiol Nutr Metab* 2008;33:997-1006.

36. Nattenmüller J, Schlett CL, Tsuchiya N, et al. Noncontrast Chest Computed Tomographic Imaging of Obesity and the Metabolic Syndrome: Part II Noncardiovascular Findings. *Journal of Thoracic Imaging* 2019;34:126-35.

37. Perthen JE, Ali T, McCulloch D, et al. Intra- and interobserver variability in skeletal muscle measurements using computed tomography images. *Eur J Radiol* 2018;109:142-146.

38. McClellan T, Allen BC, Kappus M, et al. Repeatability of Computerized Tomography–Based Anthropomorphic Measurements of Frailty in Patients With Pulmonary Fibrosis Undergoing Lung Transplantation. *Current Problems in Diagnostic Radiology* 2017;46:300-4.

39. Kim EY, Kim YS, Park I, et al. Evaluation of sarcopenia in small-cell lung cancer patients by routine chest CT. *Supportive Care in Cancer* 2016;24:4721-6.

40. Prado CM, Lieffers JR, McCargar LJ, et al. Prevalence and clinical implications of sarcopenic obesity in patients with solid tumours of the respiratory and gastrointestinal tracts: a population-based study. *The Lancet Oncology* 2008;9:629-35.

41. Sin S, Lee KH, Hur JH, et al. Impact of mediastinal lymph node enlargement on the prognosis of idiopathic pulmonary fibrosis. *PLoS ONE* 2018;13:e0201154.

42. Adegunsoye A, Oldham JM, Bonham C, et al. Prognosticating Outcomes in Interstitial Lung Disease by Mediastinal Lymph Node Assessment. An Observational Cohort Study with Independent Validation. *Am J Respir Crit Care Med* 2019;199:747-59.

43. Sgalla G, Larici AR, Golfi N, et al. Mediastinal lymph node enlargement in idiopathic pulmonary fibrosis: relationships with disease progression and pulmonary function trends. *BMC Pulm Med* 2020;20:249.

44. Grecuccio S, Sverzellati N, Uslenghi E, et al. Prognostic value of mediastinal lymph node enlargement in chronic interstitial lung disease. *Diagn Interv Radiol* 2021;27:329-335.

45. Adegunsoye A, Hrusch CL, Bonham CA, et al. Skewed Lung CCR4 to CCR6 $CD4^+$ T Cell Ratio in Idiopathic Pulmonary Fibrosis Is Associated with Pulmonary Function. *Front Immunol* 2016 Nov 23;7:516

46. Jouneau S, Crestani B, Thibault R, et al. Analysis of body mass index, weight loss and progression of idiopathic pulmonary fibrosis. *Respir Res* 2020;21:312.

47. Flaherty KR, Wells AU, Cottin V, et al. Nintedanib in Progressive Fibrosing Interstitial Lung Diseases. *N Engl J Med* 2019;381:1718-27.

48. Walsh SLF, Calandriello L, Sverzellati N, et al. Interobserver agreement for the ATS/ERS/JRS/ALAT criteria for a UIP pattern on CT. *Thorax* 2016;71:45-51.

49. Hansell DM, Goldin JG, King TE, et al. CT staging and monitoring of fibrotic interstitial lung diseases in clinical practice and treatment trials: a Position Paper from the Fleischner society. *The Lancet Respiratory Medicine* 2015;3:483-96.

50. Blanc-Durand P, Schiratti J-B, Schutte K, et al. Abdominal musculature segmentation and surface prediction from CT using deep learning for sarcopenia assessment. *Diagnostic and Interventional Imaging* 2020;101:789-94.

51. Romei C, Tavanti LM, Taliani A, et al. Automated computed tomography analysis in the assessment of idiopathic pulmonary fibrosis severity and progression. *Eur J Radiol* 2020;124:108852.

Tables

Table 1: Patients' characteristics

	All patients (n=71)	Low FFMI (n=19)	Normal or high FFMI (n=52)	P value
Clinical Data				
Age (years)	74.09 ± 7.52	76.84 ± 7.18	73.08 ± 7.46	0.062
Gender				0.010
Female	17 (23.9%)	9 (47.4%)	8 (15.4%)	
Male	54 (76.1%)	10 (52.6%)	44 (84.6%)	
Smoking history	46 (64.8%)	7 (36.8%)	39 (75.0%)	0.003
Comorbidities				
Cardiovascular disease	54 (76.1%)	12 (63.2%)	42 (80.8%)	0.207
Creatinine clearance	73.47 ± 20.58	68.57 ± 26.43	75.30 ± 17.90	0.979
Symptoms				
Cough	45 (64.3%)	13 (68.4%)	32 (62.7%)	0.659
Dyspnea				0.060
Stage 1	4 (5.6%)	2 (10.5%)	2 (3.8%)	
Stage 2	22 (31.0%)	3 (15.8%)	19 (36.5%)	
Stage 3	36 (50.7%)	9 (47.4%)	27 (51.9%)	
Stage 4	9 (12.7%)	5 (26.3%)	4 (7.7%)	
Pulmonary function tests				
FVC (% of predicted)	81.11 ± 17.49	77.74 ± 21.87	82.37 ± 15.62	0.328
DLCO (% of predicted)	46.03 ± 13.73	37.86 ± 14.64	48.42 ± 12.64	0.010
GAP index	4.21 ± 1.61	4.79 ± 1.69	4.00 ± 1.54	0.067
Nutritional status				
Clinical parameters				
BMI	27.28 ± 3.84	23.47 ± 2.79	28.67 ± 3.17	<0.001
MAMC	31.21 ± 3.39	27.76 ± 2.39	32.47 ± 2.77	<0.001
TSF	5.94 ± 3.67	5.11 ± 3.36	6.25 ± 3.77	0.247
SEFI	8.58 ± 2.15	8.35 ± 2.74	8.66 ± 1.90	0.906
Biological parameters				
Serum albumin	42.73 ± 3.03	43.00 ± 2.73	42.63 ± 3.16	0.655
Pre-albumin	0.25 ± 0.06	0.25 ± 0.05	0.25 ± 0.06	0.741
C-reactive protein	6.47 ± 8.49	7.70 ± 11.25	6.03 ± 7.35	0.732
BIA				
FMI	9.06 ± 2.34	8.67 ± 2.52	9.20 ± 2.27	0.402
Phase angle	5.26 ± 1.28	4.47 ± 0.79	5.55 ± 1.30	0.001
CT analysis				
Fibrosis score	28.30 ± 12.46	32.84 ± 11.64	26.58 ± 12.43	0.062
Emphysema score	4.19 ± 6.90	3.58 ± 4.66	4.42 ± 7.61	0.801
Lymph node enlargement	39 (56.5%)	11 (57.9%)	28 (56.0%)	0.887
Esophageal dilatation	5 (7.2%)	1 (5.3%)	4 (8.0%)	1.000
PA/AO ratio	0.83 ± 0.12	0.83 ± 0.13	0.83 ± 0.12	0.880
SMI	46.16 ± 7.79	40.14 ± 6.95	48.36 ± 6.91	<0.001

index
FVC = forced vital capacity
DLCO = carbon monoxide diffusing capacity
GAP index = Gender-Age-Physiology index
BMI = body mass index
MAMC = mid-arm circumference
TSF = triceps skinfold thickness
SEFI = Simplified Evaluation of Food Intake
BIA = bioelectrical impedance analysis
FMI = fat mass index
SMI = skeletal muscle index
PA/AO ratio: main pulmonary artery to ascending aorta diameter ratio

FFMI = fat-free mass

Table 2: Correlation between SMI and parameters of nutritional and respiratory status

Variable	Correlation Coefficient	P value
BMI	0.579	<0.001
MAMC	0.497	<0.001
TSF	0.198*	0.101
SEFI	-0.156*	0.197
Albumin	-0.171	0.157
Pre-albumin	-0.048	0.708
CRP	-0.062	0.624
FFMI	0.637	<0.001
FMI	0.170	0.156
Phase angle	0.229	0.054
FVC	0.163	0.177
DLCO	0.347	0.006
Fibrosis score	-0.019	0.879
Emphysema score	-0.016	0.899

BMI = body mass index
MAMC = mid-arm circumference
TSF = triceps skinfold thickness
SEFI = Simplified Evaluation of Food Intake
CRP = C-reactive protein
FFMI = fat-free mass index
FMI = fat mass index
FVC = forced vital capacity
DLCO = carbon monoxide diffusing capacity

Table 3: Diagnostic performance of SMI for low FFMI

	Optimal threshold	Sensitivity	Specificity	Positive Predictive Value	Negative Predictive Value	AUC
Male Diagnostic Performance	SMI ≤ 47.4 cm^2/m^2	80% [55.2%;100%]	63.64% [49.4%;77.9%]	33.33% [14.5%;52.2%]	93.33% [84.4%;100%]	0.75 [0.59;0.92]
Female Diagnostic Performance	SMI ≤ 35 cm^2/m^2	55.56% [23.1%;88%]	87.5% [64.6%;100%]	83.33% [53.5%;100%]	63.64% [35.2%;92.1%]	0.79 [0.56;1.00]
Overall Diagnostic Performance	SMI ≤ gender-based threshold	78.95% [60.6%;97.3%]	69.23% [56.7%;81.8%]	48.39% [30.8%;66%]	90% [80.7%;99.3%]	0.80 [0.68;0.91]

SMI = skeletal muscle index

Table 4: Variables associated with death or transplantation

	Univariate analysis HR [95% CI]	P value	Multivariate analysis HR [95% CI]	P value
Age	1.12 [1.03 ; 1.22]	0.008		
Gender (male)	1.93 [0.44 ; 8.42]	0.383		
FVC	0.95 [0.92 ; 0.98]	0.001		
DLCO	0.92 [0.88 ; 0.97]	0.003	0.92 [0.86 ; 0.99]	0.026
BMI	0.89 [0.78 ; 1.01]	0.080		
SMI ≤ threshold	2.20 [0.88 ; 5.51]	0.091		
Fibrosis score	1.05 [1.01 ; 1.09]	0.007		
Emphysema score	0.88 [0.74 ; 1.04]	0.129		
Lymph node enlargement	1.91 [0.72 ; 5.06]	0.195		
Esophageal dilatation	0.95 [0.12 ; 7.17]	0.957		
PA/AO ratio (0.1 unit)	1.33 [0.92 ; 1.93]	0.127		

Univariate analysis: number of patients, 67; number of events, 20
Multivariate analysis: number of patients, 55; number of events, 14
FVC = forced vital capacity
DLCO = carbon monoxide diffusing capacity
BMI = body mass index
SMI = skeletal muscle index measured at L1 level. Thresholds were 47.4 and 35 cm^2/m^2 for male and female, respectively
PA = Pulmonary Artery
AO = Aorta

Table 5: Variables associated with hospitalization

	Univariate analysis HR [95% CI]	P value	Multivariate analysis HR [95% CI]	P value
Age	1.02 [0.96 ; 1.08]	0.507		
Gender (male)	0.81 [0.32 ; 2.03]	0.650		
FVC	0.98 [0.96 ; 1.01]	0.167		
DLCO	0.96 [0.93 ; 0.99]	0.020		
BMI	0.94 [0.84 ; 1.04]	0.225		
SMI ≤ threshold	1.55 [0.70 ; 3.40]	0.276		
Fibrosis score	1.03 [1.00 ; 1.07]	0.039	1.05 [1.01 ; 1.08]	0.0078
Emphysema score	0.96 [0.89 ; 1.04]	0.357		
Lymph node enlargement	2.93 [1.16 ; 7.41]	0.023		
Esophageal dilatation	1.50 [0.35 ; 6.44]	0.582		
PA/AO ratio (0.1 unit)	1.51 [1.09 ; 2.09]	0.014	1.53 [1.13 ; 2.07]	0.0065

Univariate analysis: number of patients, 67; number of events, 25
Multivariate analysis: number of patients, 64; number of events, 24
FVC = forced vital capacity
DLCO = carbon monoxide diffusing capacity
BMI = body mass index
SMI = skeletal muscle index measured at L1 level. Thresholds were 47.4 and 35 cm^2/m^2 for male and female, respectively
PA = Pulmonary Artery
AO = Aorta

Legends of Figures

Figure 1. Representative CT images of the sequential steps for skeletal muscle index (SMI) segmentation. Cross-sectional CT slice at the level of the first lumbar vertebra (A). Application of a thresholding algorithm keeping the pixels between -29 and 150 Hounsfield Units (B). Manual segmentation of skeletal muscle (C). Final skeletal muscle area allowing the calculation of the SMI (D).

Figure 2. Flowchart of the study.

Figure 3. Graph showing interobserver agreement of SMI. The means of SMI measurements of observers 1 and 2 are plotted against their difference according to Bland-Altman analysis.

Figure 4. Receiver operating characteristic curve for skeletal muscle index (SMI) in prediction of a low fat-free mass index (FFMI).

Figure 5. Chest CT examination of a 72-year-old man with idiopathic pulmonary fibrosis who died 6 months after diagnosis. Axial CT image at T10 level (A) shows subpleural predominant reticular abnormality (arrows) and traction bronchiectasis (arrowhead), without honeycombing. The fibrosis score was evaluated at 23%. Axial CT image at L1 level (B) after skeletal muscle segmentation shows a calculated SMI of 28.9 cm^2/m^2.

Figure 6. Chest CT examination of a 78-year-old man with idiopathic pulmonary fibrosis who was still alive 29 months after diagnosis. Axial CT image at T10 level (A) shows subpleural predominant reticulation, extensive honeycombing (arrows), traction bronchiectasis (arrowheads), and architectural distortion. The fibrosis score was evaluated at 50%. Axial CT image at L1 level (B) after skeletal muscle segmentation shows a calculated SMI of 56.2 cm^2/m^2.

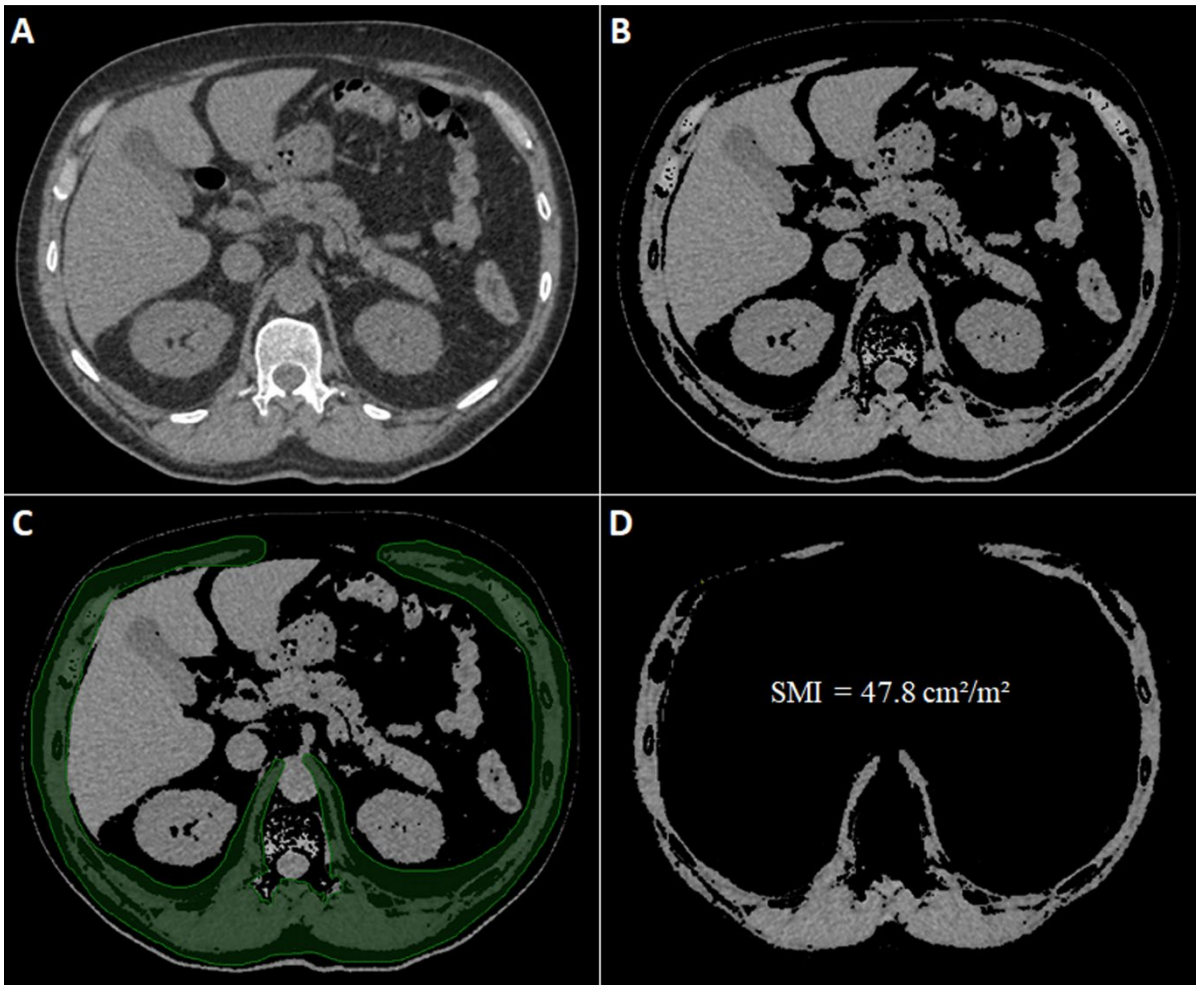
A
B
C
D
SMI = 47.8 cm²/m²

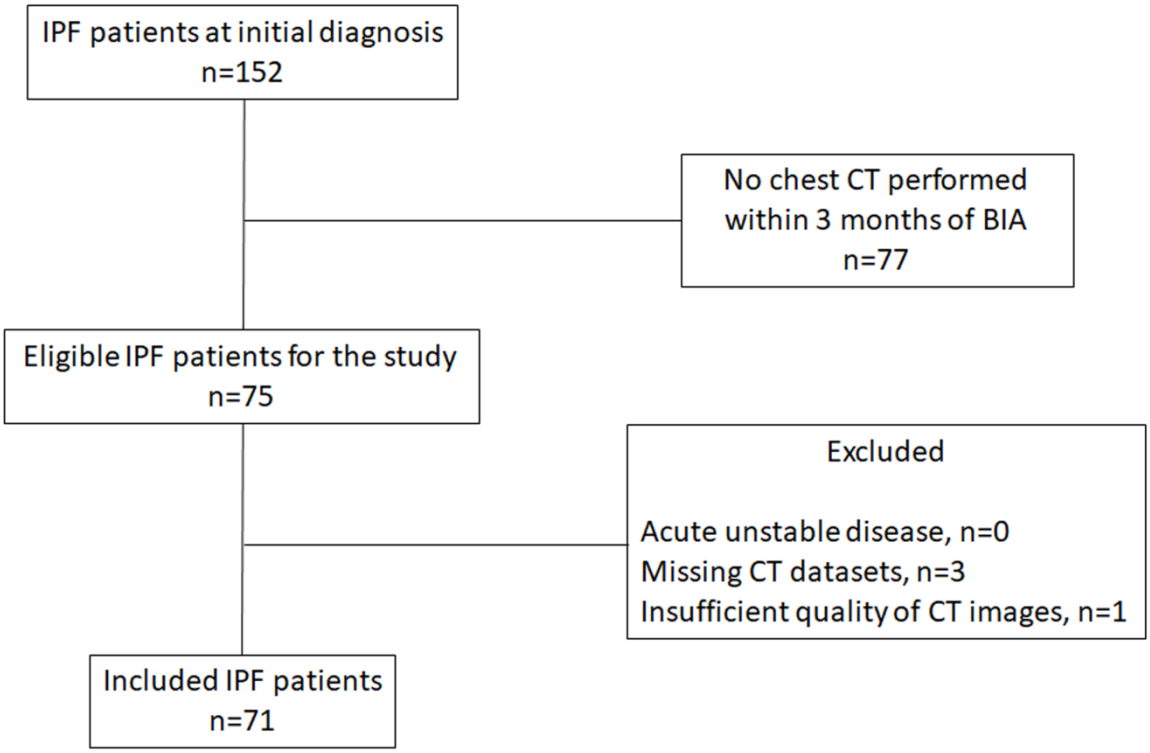
IPF patients at initial diagnosis
n=152
No chest CT performed
within 3 months of BIA
n=77
Eligible IPF patients for the study
n=75
Excluded
Acute unstable disease, n=0
Missing CT datasets, n=3
Insufficient quality of CT images, n=1
Included IPF patients
n=71

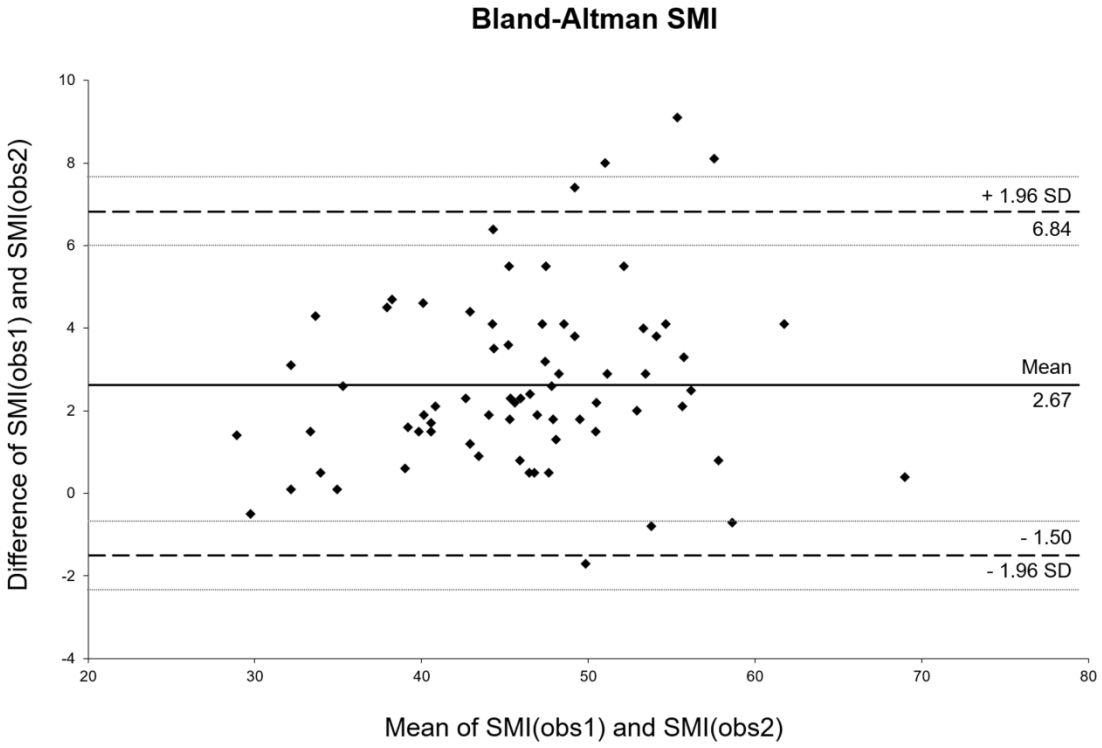
Bland-Altman SMI
Difference of SMI(obs1) and SMI(obs2)
Mean of SMI(obs1) and SMI(obs2)
+ 1.96 SD
6.84
Mean
2.67
- 1.50
- 1.96 SD
10
8
6
4
2
0
-2
-4
20
30
40
50
60
70
80

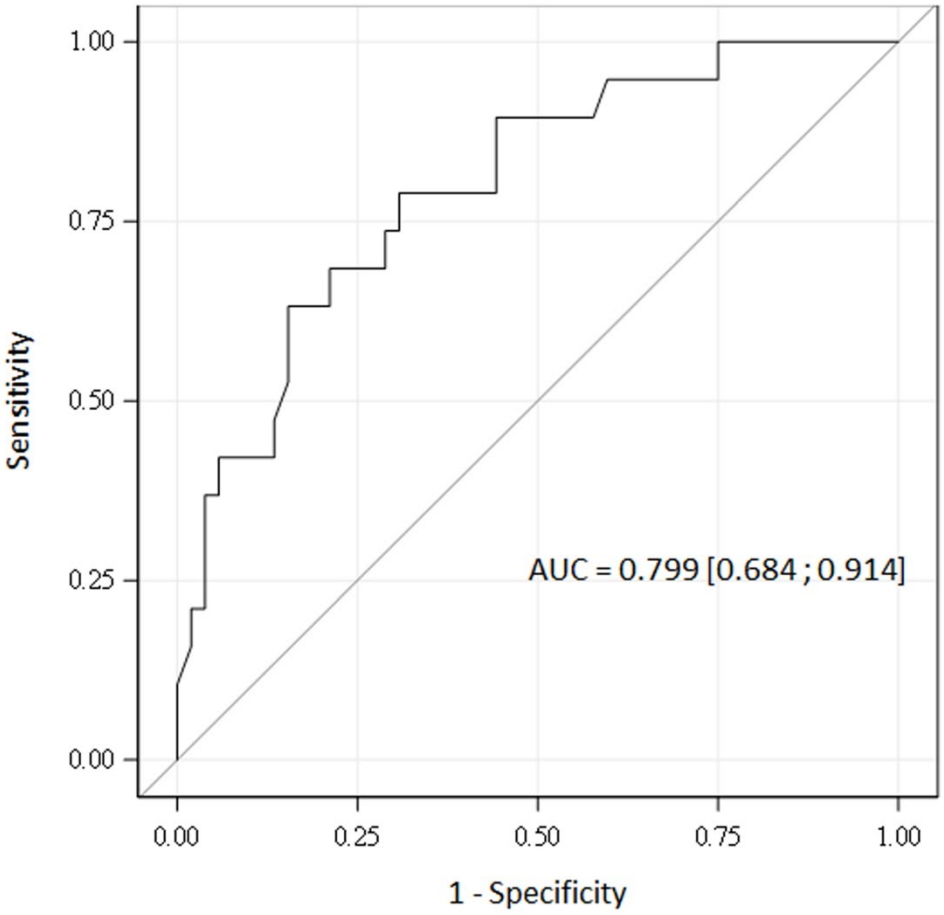
1.00
0.75
0.50
0.25
0.00
Sensitivity
0.00
0.25
0.50
0.75
1.00
1 - Specificity
AUC = 0.799 [0.684 ; 0.914]

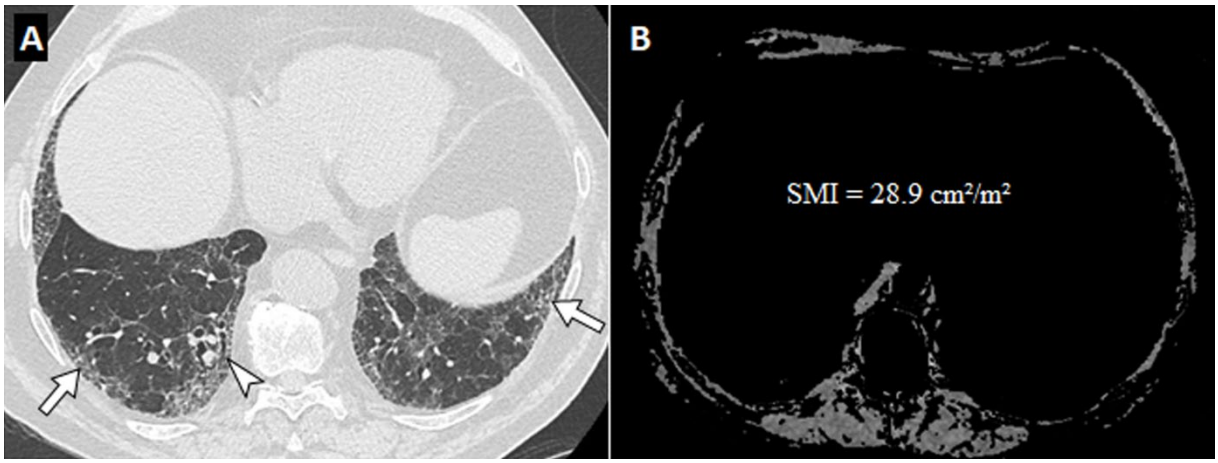
A
B
SMI = 28.9 cm²/m²

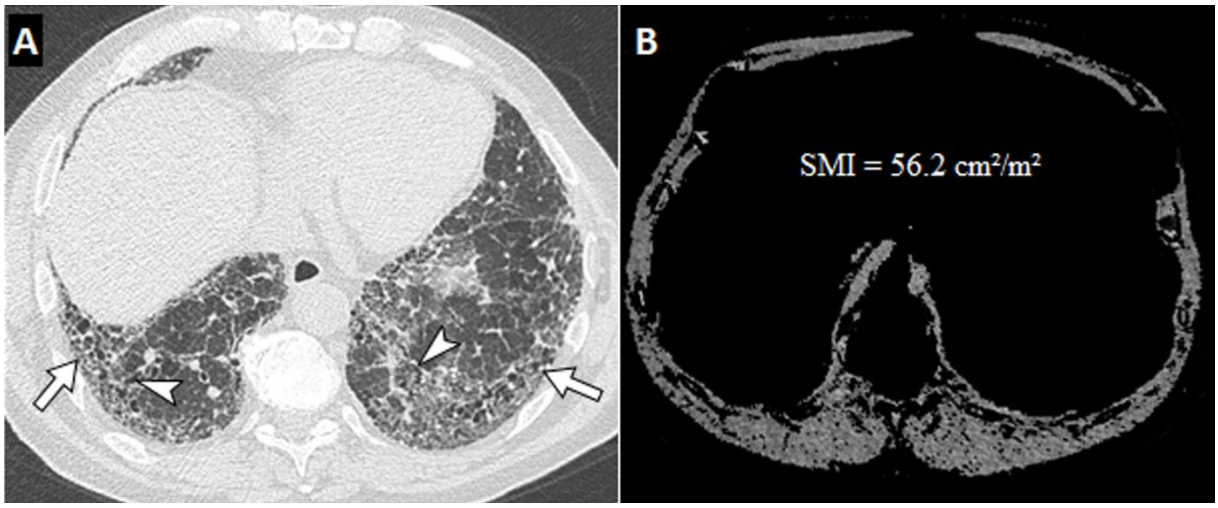
A
B
SMI = 56.2 cm²/m²